# Short Papers

## S Matrix of Slot-Coupled H-Plane Tee Junction Using Rectangular Waveguides

B. N. DAS, A. CHAKRABORTY,
AND N. V. S. NARASIMHA SARMA

*Abstract*—**Complex scattering matrix parameters of a slot-coupled waveguide tee junction are determined using a moment method of analysis with entire orthogonal basis functions and including a rigorous analysis of the effect of wall thickness. The variations of the equivalent network parameter, coupling, and return loss with frequency are evaluated and the results are compared with experimental data. The unitary property of the $S$ matrix is verified. The dependence of coupling on slot length, slot width, and thickness is presented.**

### I. Introduction

Considerable limitations in evaluating the equivalent circuit of the slot-coupled $H$-plane tee junction [1] have been found. The method does not permit a rigorous analysis of the effect of wall thickness and evaluation of $S$ parameters.

In the present work, an analysis is carried out using the moment method with entire basis functions which permits the inclusion of finite wall thickness and the evaluation of corresponding $S$ parameters. The formulation suggested by Josefsson [2] for a radiating slot is suitably modified to evaluate the parameters of the $S$ matrix, the coupling, and the impedance presented by the junction to the feed waveguide.

### II. Coupling, Scattering Matrix Elements, and Network Parameters

Consider an $H$-plane rectangular waveguide tee junction coupled through a longitudinal slot on the narrow wall. In order to take the effect of wall thickness into account, the coupling slot is considered as a section of a waveguide between two interfaces: 1) between the primary rectangular waveguide and the stub waveguide (interface $C$) and 2) between the stub waveguide and the tee arm (interface $D$).

From the boundary conditions at the two interfaces, following the method suggested in the literature [2], amplitude coefficients of the slot field, expressed as a superposition of sinusoidal basis functions, are determined. The expressions for the elements of the matrices used are presented in the Appendix.

The expressions for $H_z^{\text{b.s.}}$, the dominant-mode magnetic field backscattered toward the input port, and $H_z^{\text{f.s}}$, the dominant-mode magnetic field scattered toward the output port, of the feed waveguide are derived using [4, eqs. (7-31) and (7-34)]. The reflection and transmission coefficients are obtained as

$$\Gamma = S_{11} = S_{22} = \frac{H_z^{\text{b.s.}}}{H_z^{\text{inc}}} = \sum_r E_r \frac{rw\left(k^2-\beta^2\right)\left(e^{j\beta L}-(-1)^r e^{-j\beta}\right)}{j\beta L\sqrt{\frac{2a}{b}}\left(\left(\frac{r\pi}{2L}\right)^2-\beta^2\right)} \tag{1}$$

and

$$T = S_{12} = S_{21} = 1+\frac{H_z^{\text{f.s.}}}{H_z^{\text{inc}}} = 1-\sum_r E_r \frac{rw\left(k^2-\beta^2\right)\left(e^{-j\beta L}-(-1)^r e^{j\beta L}\right)}{j\beta L\sqrt{\frac{2a}{b}}\left(\beta^2-\left(\frac{r\pi}{2L}\right)^2\right)} \tag{2}$$

where the $E_r$'s are the elements of the matrix of the amplitude coefficients at interface $C$.

Using [3, eq. (8-40)] and the slot field at interface $D$, the dominant-mode modal voltage in the tee arm is obtained as

$$V_{10}^e = \sqrt{\frac{2}{ab}}\sum_q E_q 2w \frac{q\pi/2L}{\left[\left(\frac{q\pi}{2L}\right)^2-\left(\frac{\pi}{b}\right)^2\right]} \cdot \begin{bmatrix} -2\cos\frac{\pi L}{b}, & q \text{ odd} \\ 0, & q \text{ even} \end{bmatrix} \tag{3}$$

where the $E_q$'s are given by the elements of the matrix of the amplitude coefficients at interface $D$.

Since the modal voltage of the incident wave is unity, coupling from the primary guide to the secondary guide is given by

$$C = S_{13} = S_{23} = S_{31} = S_{23} = V_{10}^e \tag{4}$$

$$C_{\text{dB}} = 20\log|V_{10}^e|.$$

*Reflection Coefficient Seen from the Tee Arm*

When the junction is excited at the tee arm and other ports are match terminated, matching the boundary conditions and following a similar procedure, the total tangential field at interface $D$ is of the form

$$[E] = 2\{[I]+[B][G^{(1)}]^{-1}[h^{(1)}][B]\}\{[G^{(2)}]^{-1}[h^{(2)}][B][G^{(1)}]^{-1}[h^{(1)}][B]-[I]\}^{-1}[G^{(2)}]^{-1}[h_2^{\text{inc}}]. \tag{5}$$

Manuscript received September 27, 1988; revised November 30, 1989.
The authors are with the Department of Electronics and Electrical Communication Engineering, Indian Institute of Technology, Kharagpur, 721 302 India.
IEEE Log Number 9034895.

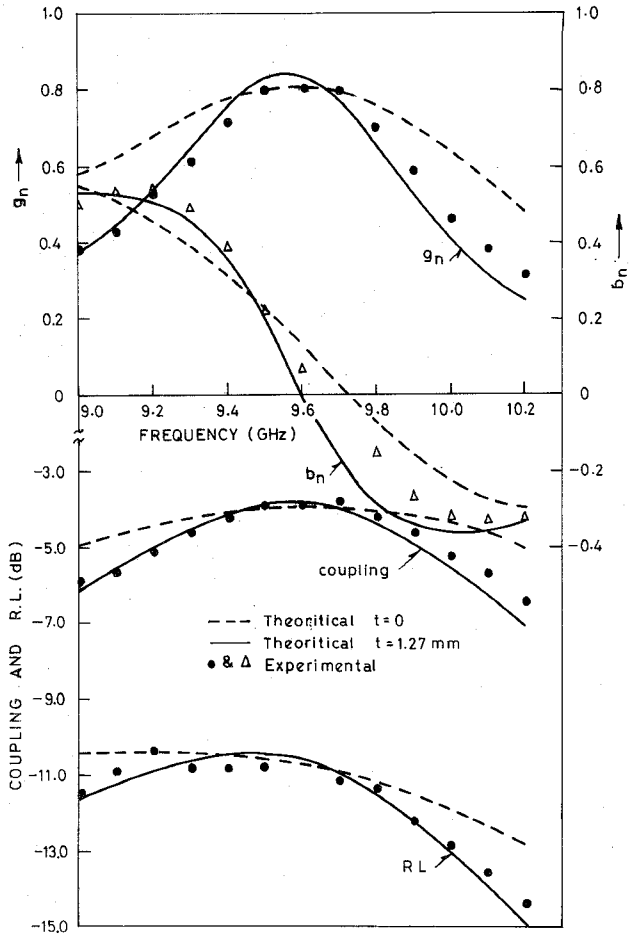


Fig. 1. Variation of coupling, VSWR, normalized conductance, and normalized susceptance with frequency for $2L = 16$ mm, $2W = 0.8$ mm, and $t = 1.27$ mm.

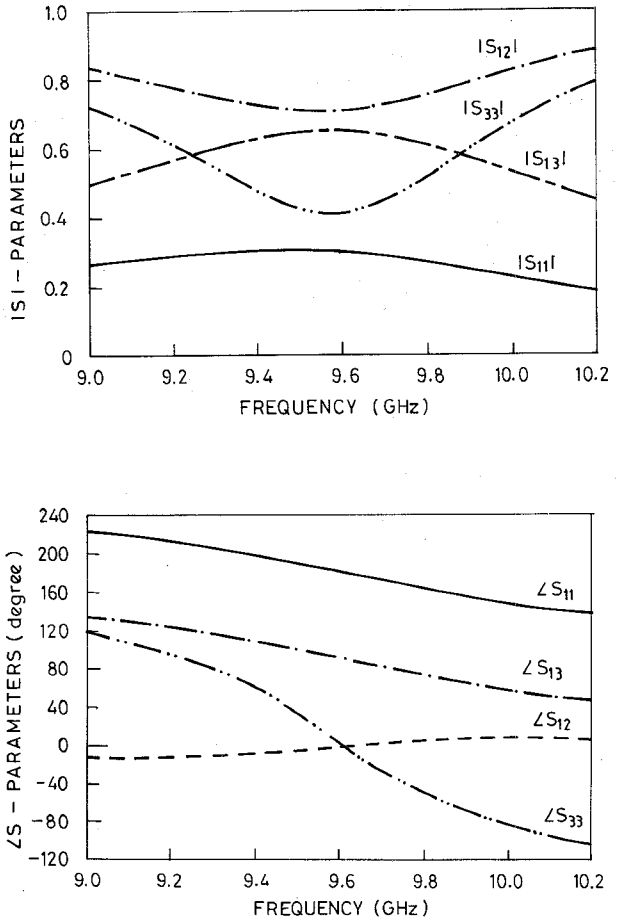


Fig. 2. Variation of $S$ parameters with frequency.

For an incident magnetic field of the form

$$H_{z2}^{\text{inc}} = \frac{\beta}{\omega\mu}\sqrt{\frac{2}{ab}}\cos\frac{\pi z}{b}$$

the elements of the column matrix $[h_2^{\text{inc}}]$ are

$$h_{2s}^{\text{inc}} = \langle H_{z2}^{\text{inc}}, e_s\rangle = \frac{\beta}{\omega\mu}\sqrt{\frac{2}{ab}}\,2w\frac{s\pi/2L}{\left(\frac{s\pi}{2L}\right)^2-\left(\frac{\pi}{b}\right)^2}\cdot\begin{bmatrix}2\cos\dfrac{\pi L}{b}, & s \text{ odd}\\ 0, & s \text{ even}\end{bmatrix}. \quad (6)$$

From the expression for the dominant-mode backscattered electric field derived by following the procedure suggested in [3, sec. 8-2], the reflection coefficient seen from the tee arm is obtained as

$$\Gamma_s = S_{33} = -1+\frac{E_x^{\text{b.s.}}}{E_x^{\text{inc}}} = -1-\sum_v E_v\frac{2w\left(\sqrt{2/ab}\right)v\pi/2L}{\left(\frac{v\pi}{2L}\right)^2-\left(\frac{\pi}{b}\right)^2}\cdot\begin{bmatrix}2\cos\dfrac{\pi L}{b}, & v \text{ odd}\\ 0, & v \text{ even}\end{bmatrix} \quad (7)$$

where the $E_v$'s are the elements of column matrix $[E]$ of (5). Since the junction is lossless, the $S$ matrix is unitary. The normalized lumped shunt admittance producing the reflection coefficient $\Gamma$ looking from the input port is given by

$$Y = g + jb = -2\Gamma/(1.+\Gamma). \quad (8)$$

## III. Numerical and Experimental Results

Using (1), (4), and (8), variations of coupling, return loss, normalized conductance, and normalized susceptance are evaluated for slot length $2L = 16$ mm, $2W = 0.8$ mm, and $t = 1.27$ mm over the frequency band 9–10.2 GHz. Theoretical and experimental data are presented in Fig. 1. The values of $g$ and $b$ are determined experimentally from measured data on the magnitudes of coupling and reflection coefficients based on their relation with $g$ and $b$; a HP8410B network analyzer is used in view of the inaccuracy in measuring the phase of the reflection coefficient. Using (1)–(4) and (7), $S$ parameters are evaluated and the results are presented in Fig. 2. From these numerical results, the unitary property of the $S$ matrix has been verified. A complete analysis of varying $L$, $W$, and $t$ is also added. Figs. 3 and 4 present corresponding numerical data.

## IV. Discussion

Reasonable agreement between theoretical and experimental results has been obtained for coupling and return loss. Figs. 3 and 4 show that the maximum coupling coefficient which occurs at resonance decreases as the slot width increases. This is due to

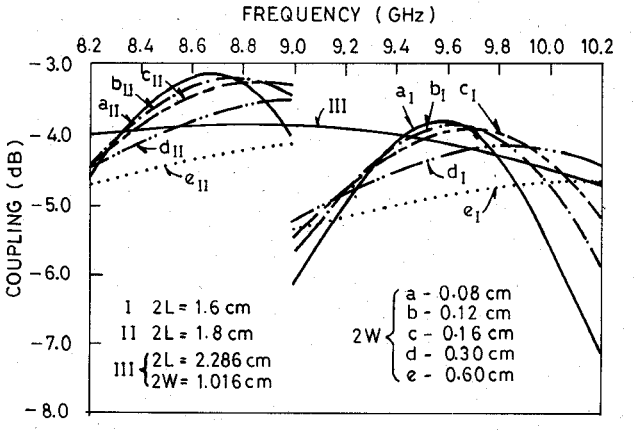


Fig. 3. Variation of coupling with frequency for different slot widths and slot lengths.

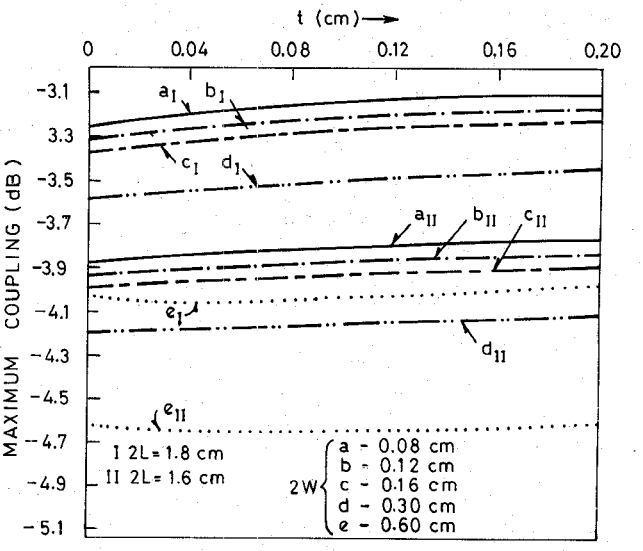


Fig. 4. Variation of maximum coupling with thickness for different slot widths and slot lengths.

the fact that as the slot width is increased past the value where the resonant conductance is unity, the strong reflection by the slot in the feed waveguide results in a reduction in maximum coupling as the slot width increases. On the other hand, when the slot width is narrow and resonant conductance is less than unity, maximum coupling increases with an increase in slot width. Slot conductance increases as the slot width increases. This accounts for higher value of $g$ near resonance for a thick wall.

## Appendix

Using [4, eqs. (7-31) and (7-34)], an expression for $H_z^{(1)}$ is obtained. Taking the inner product of $H_z^{(1)}$ with the testing function and using the above equations, expressions for $G^{(1)}$ and $h^{(1)}$ are obtained:

$$G_{sp}^{(1)}/h_{si}^{(1)} = \pm \sum_m \sum_n \frac{\epsilon_m \epsilon_n}{2\gamma ab} \left( \frac{2w \cos\frac{n\pi}{2} \sin\frac{n\pi w}{a}}{n\pi w/a} \right)^2 \cdot \frac{(1/j\omega\mu)}{\gamma^2 + \left(\frac{j\pi}{2L}\right)^2} \cdot \left[ \left(k^2+\gamma^2\right) \frac{j\pi}{2L} e^{-\gamma L} \frac{(s\pi/2L)}{\gamma^2 + \left(\frac{s\pi}{2L}\right)^2} \cdot \left\{ -\left(e^{\gamma L} - e^{-\gamma L}(-1)^s\right) - (-1)^j \left(e^{-\gamma L} - (-1)^s e^{\gamma L}\right) \right\} + \left(k^2 - \left(\frac{j\pi}{2L}\right)^2\right) 2L\gamma_{mn}\delta_{js} \right] + Y_j 2Lw\delta_{js}$$

where

$$\delta_{js} = \begin{cases} 1 & \text{for } s = j \\ 0 & \text{for } s \neq j \end{cases}$$

$$- \text{ for } p \text{ and } + \text{ for } i, \qquad j = p, i.$$

An expression for $H_z^{(2)}$ is obtained from [3, p. 390, eq. (8-39)]. Taking the inner product of $H_z^{(2)}$ with the testing function and using the above equations, elements of the matrices $G^{(2)}$ and $h^{(2)}$ are obtained:

$$G_{sp}^{(2)}/h_{si}^{(2)} = \pm \sum\sum \left( \frac{\epsilon_m \epsilon_n Y_0^e m^2}{b^2} + \frac{4Y_0^m n^2}{a^2} \right) \left[ \frac{ab}{\{(ma)^2 + (nb)^2\}} \right] \cdot \left( \frac{2w \cos\frac{n\pi}{2} \sin\frac{n\pi w}{a}}{(n\pi w/a)} \right)^2 \frac{(j\pi/2L)}{(j\pi/2L)^2 - (m\pi/b)^2} \cdot \left[ (-1)^j \sin\left(\frac{m\pi L}{b} + \frac{m\pi}{2}\right) + \sin\left(\frac{m\pi L}{b} - \frac{m\pi}{2}\right) \right] \cdot \frac{(s\pi/2L)}{(s\pi/2L)^2 - (m\pi/b)^2} \cdot \left[ (-1)^s \sin\left(\frac{m\pi L}{b} + \frac{m\pi}{2}\right) + \sin\left(\frac{m\pi L}{b} - \frac{m\pi}{2}\right) \right]$$

where

$$Y_0^e = \frac{\gamma}{j\omega\mu} \quad \text{and} \quad Y_0^m = \frac{j\omega\epsilon}{\gamma}$$

$$+ \text{ for } p \text{ and } - \text{ for } i, \qquad j = p, i$$

and $\epsilon_m, \epsilon_n$ are Neumann numbers.

## Acknowledgment

The authors would like to express their thanks to the IEEE reviewers for their very useful suggestions.

## References

[1] V. M. Pandharipande and B. N. Das, "Equivalent circuit of a narrow wall waveguide slot coupler," *IEEE Trans. Microwave Theory Tech.*, vol. MTT-27, pp. 800–804, Sept. 1979.

[2] L. G. Josefsson, "Analysis of longitudinal slots in rectangular waveguides," *IEEE Trans. Antennas Propagat.*, vol. AP-35, pp. 1351–1357, Dec. 1987.

[3] R. F. Harrington, *Time-Harmonic Electromagnetic Fields*. New York: McGraw Hill, 1961.

[4] G. Markov, *Antennas*. Moscow: Progress Publishers, 1965.